

Algorithmic Design of On-chip mm-wave Slow-wave Quadrature Coupler in Silicon Technology

Dristy Parveg, *Student Member, IEEE*, Mikko Varonen, Denizhan Karaca, Mohsin Khan, Ali Vahdati, and Kari Halonen, *Member, IEEE*

Abstract—In this paper, we have presented an algorithmic design methodology for designing integrated millimeter-wave quadrature coupler based on slow-wave coupled line. The design methodology is verified by a 3-dB quadrature coupler in a commercially available CMOS technology. The designed CMOS coupler covers the whole E- to W-band and occupies only 0.0115 mm² silicon area. The consumed wafer area is 50% smaller compared to the conventional microstrip line based couplers. Measurement of the slow-wave 90° coupler shows a -3.5 dB through and -4.4 dB coupling at 90 GHz, and less than ±1-dB amplitude and ±4° phase errors from 55 to 110 GHz.

Index Terms—Coupler, coupled line, CMOS, E-band, millimeter-wave, slow-wave, quadrature, W-band, 3-dB coupling.

I. INTRODUCTION

COMMUNICATION at millimeter-wave frequencies has drawn a lot of consideration due to the availability of wide fractional bandwidths and small antenna sizes. Recently, there has been increasing research and commercial development of integrated circuits for wireless communication at E- and W-band and automotive radar application at 77 GHz. Commercially available silicon technologies show potentiality to realize cost-effective, highly integrated systems for these applications [1]–[3]. Like in microwave design techniques, silicon IC designs at millimeter-wave frequencies also include transmission lines, splitters, combiners, baluns, and couplers [Floyd1], [Niknjad], [Mikko.RMixer]. Among these passive circuit elements, 3-dB coupler having 90° phase difference between the outputs is a very important building block. It can be used for I/Q modulator-demodulator [ISSCC.shimawaki], phase shifters [IBM.60G], triplers [Northop.tripler], and various mixer topologies [D.MWCL], [Rebeiz.mixer]. These couplers are usually realized by the design technique called Lange

coupler, invented by J. Lange [MKK.6]. The Lange couplers are popular due to its broadband and accurate quadrature performance. The coupler design techniques involve quarter wavelength lines at the design frequency and are usually realized with microstrip lines. One major drawback to microstrip lines on the standard silicon technologies is the low effective dielectric constant (~ 4) which is defined by the surrounding media (silicon dioxide). Therefore, the sizes of the couplers become very large.

Efforts have been given to miniaturize the size of silicon quadrature couplers [Floyd.IMS], [EuMIC.Ferrari]. In [Floyd.IMS], thin film microstrip line was used to achieve the required coupling coefficient and an aggressive meandering was implemented to reduce the size of the coupler. In [EuMIC.Ferrari], coupler based on coupled slow-wave coplanar waveguide (CS-CPW) was presented and required coupling was achieved by modifying the shielding ribbons. However, the work has considered BiCMOS technology which allowed the designers to use wider lines compared with a standard CMOS technology. Furthermore, none of the works did address the modeling methodology used for designing their proposed complex structures.

In this work, an algorithmic design technique for a compact mm-wave coupler is presented which is feasible for any silicon technology. The coupler design is based on the use of CS-CPW and approaches a complete new way to miniaturize the structure. The proposed structure is easy to model and scalable in length. The structure provides required coupling by placing metal slabs on coupled lines within the CS-CPW structure. Since the coupler structure is based on CS-CPW structure, the modeling of the coupler relies on the fast and reliable modeling technique proposed in [Dristy.EuMIC]. Furthermore, the behavior of a CS-CPW is analyzed and based on the analysis; a conclusion of defining a good initial value of the design parameters for the EM simulation is drawn. For a proof-of-concept, a 3-dB quadrature coupler was designed. The coupler exhibits excellent performance over the entire E- to W-band.

The paper is organized as follows. Section II describes briefly the modeling methodology of the CS-CPWs. A study on the behavior of CS-CPW is covered in section III. A mathematical model is derived in section IV from the behavior analysis to estimate the initial design parameters for the EM simulation. An algorithmic design of the coupler based on CS-CPW is presented in section V. Section VI includes the design detail of the 3-dB quadrature coupler. Measurement results are presented in section VII.

Manuscript received in May 15, 2017, revised in September 15, 2017, and accepted in October 15, 2017. This work was supported by the Academy of Finland through the FAMOS project and Postdoctoral Researcher funding and Finnish Funding Agency for Innovation (Tekes) under the 5WAVE project.


D. Parveg and K. A. I. Halonen are with the Department of Electronics and Nanoengineering, Aalto University, 02150 Espoo, Finland (email: dristy.parveg@aalto.fi).

M. Varonen was with the Department of Electronics and Nanoengineering, Aalto University. He is currently with Technical Research Centre of Finland, VTT, 02150 Espoo, Finland (email: mikko.varonen@vtt.fi).

D. Karaca, was with the Department of Electronics and Nanoengineering, Aalto University. He is currently with ICEEYE OY, 02150 Espoo, Finland (email: denizhan.karaca@iceeye.com).

M. Khan is with the Department of Computer Science, University of Helsinki, Helsinki, Finland (email: mohsin.khan@helsinki.fi).

A. Vahdati, was with the Department of Electronics and Nanoengineering, Aalto University. He is currently with Ericsson AB, Kista, Sweden (email: ali.vahdati@ericsson.com).

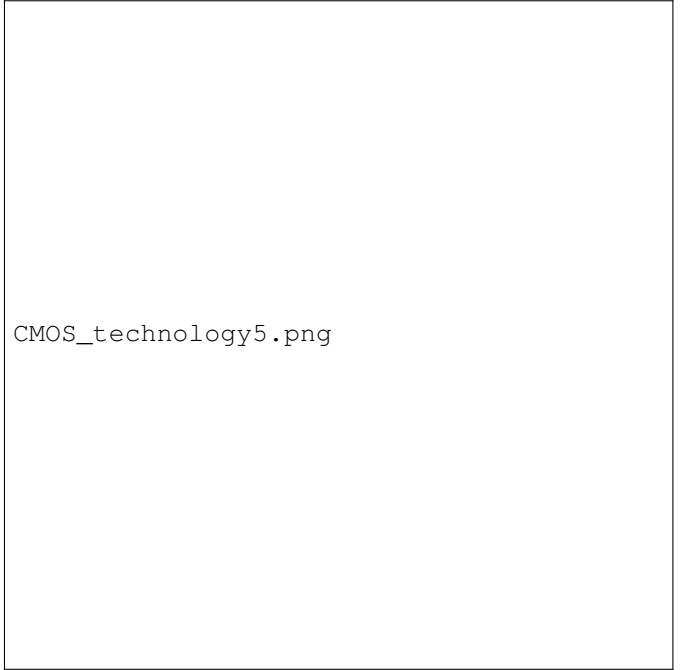


CS-CPW_basic.png

Fig. 1. 3-D view of a coupled slow-wave coplanar waveguide (CS-CPW).

II. MODELING OF THE COUPLED SLOW-WAVE CO-PLANAR WAVEGUIDE

A coupled slow-wave co-planar waveguide (CS-CPW) is an efficient way of implementing a coupled line in silicon technology. The CS-CPW are basically the modified versions of slow-wave co-planar waveguides (S-CPWs) which are popular for their compactness [J.Long], [Ferrari2]. 3-D view of a fundamental CS-CPW is illustrated in Fig. 1. The CS-CPW structures are composed of two signal lines of widths W separated by a gap S , two side-ground lines with widths of GW located in a distance of SG from the signal lines, and slotted metal strips below the signal lines at a distance of D . Simulation of the complete CS-CPW structure as in Fig. 1 is computationally heavy and time-consuming. Therefore, an efficient modeling methodology for designing the CS-CPW is proposed in [D.EuMIC] and successfully verified in [D. TMTT]. In the modeling approach, the side-ground lines serve as well-defined ground return current paths for the even-mode signal propagation and divides the EM problem into four parts [D.EuMIC]. The EM problem is first divided into odd- and even-mode analysis and each mode is further decoupled into odd- and even-mode R & L and C & G analysis. Here the R , L , C , and G are the typical transmission line parameters (Telegraphers equation) [Pozar] which support the transverse electromagnetic (TEM) propagation. A graphical representation of the modeling method is illustrated in Fig. 2. The port definitions for the EM simulations of the odd- and even-mode analysis are also included in the Fig. 2. Four two-port S -parameter data sets are obtained from these four EM simulations. Using these data sets, the odd- and even-mode R , L , C , and G parameters are calculated by the formulas stated in [Einstad]. Once the R , L , C , and G parameters for both the modes are obtained, the other essential transmission



CMOS_technology5.png

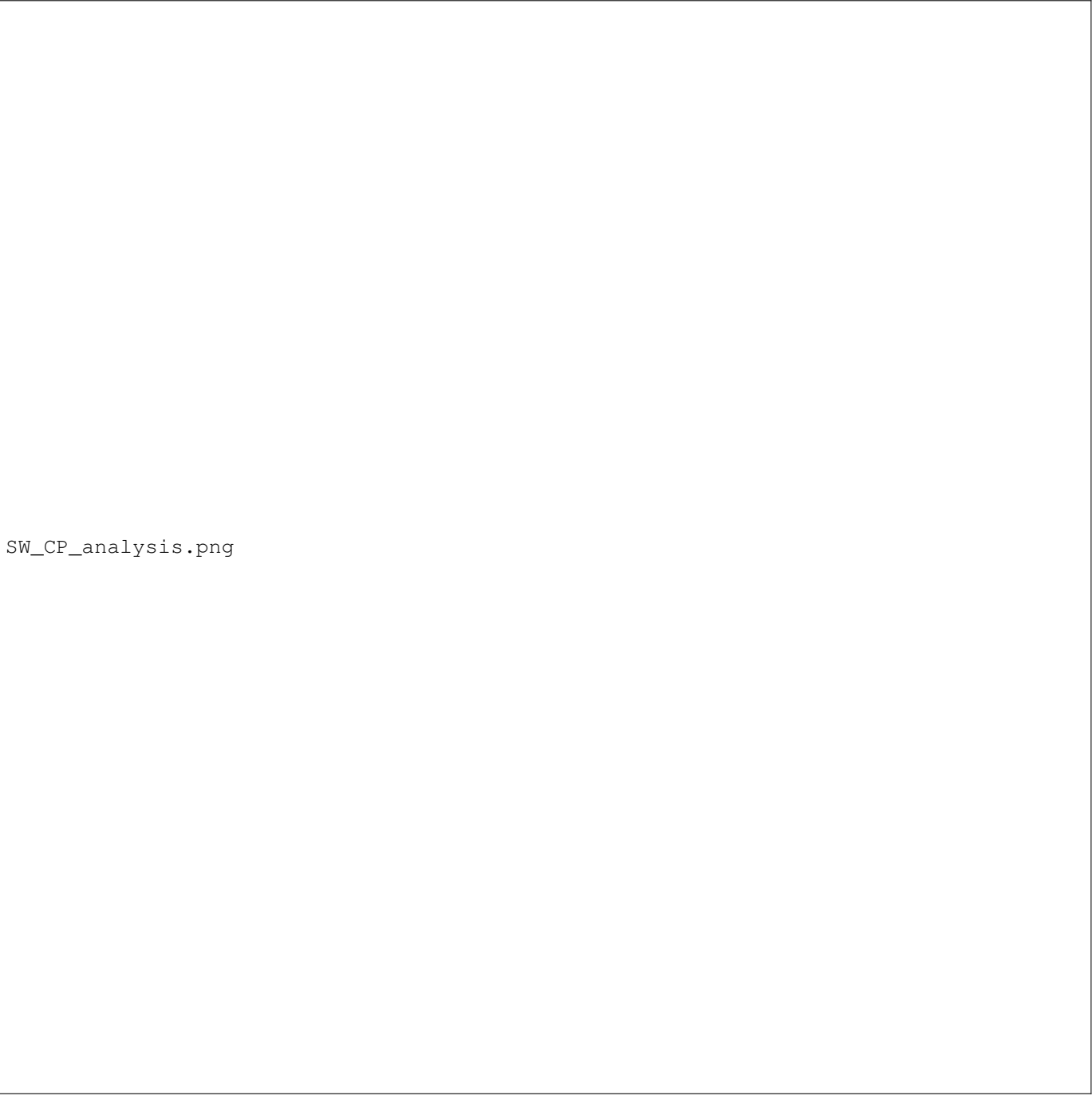
Fig. 3. A generic cross-sectional view of the applied CMOS technology and a CS-CPW structure.

line parameters can be calculated from [Pozar]. The necessary model parameters for a coupled transmission line are odd- and even-mode characteristic impedances (Z_{0o} , Z_{0e}), effective dielectric constants (ϵ_{ro} , ϵ_{re}), attenuation constants (α_o , α_e), and loss tangent ($\tan\delta$). To design a scalable (in length) electrical model of the CS-CPW, a physical coupled line model (CLINP) supported by the simulator Keysight's ADS [ADS] is used. A first-order frequency-dependent loss model is considered in the line model.

III. BEHAVIOR ANALYSIS OF COUPLED SLOW-WAVE CO-PLANAR WAVEGUIDES

In this section, we have analyzed the electrical behavior of the CS-CPW structure by EM simulations. We have studied the structure, mainly to derive a table showing the behavior of the structure at different geometric parameters. This table will help the designers to select the suitable initial values of the geometric parameters for the EM simulations in order to obtain a given design goal. Furthermore, the table will also be useful for the optimization iterations of the design. For this study, we had varied the geometric parameters S , D , W , SG , GW and observed the changes in odd- and even-mode inductances (L_{odd} , L_{even}), capacitances (C_{odd} , C_{even}), and impedances (Z_{0o} , Z_{0e}). While varying one parameter, the other parameters were kept constant. A commercially available standard 65-nm CMOS technology was used and we have considered a length of $110 \mu\text{m}$ of CS-CPW for this analysis. The EM simulations were performed based on the modeling methodology described in the previous section. A generic cross-sectional view of the CMOS technology applied in this study is shown in Fig. 3.

At first we had created a CS-CPW structure with the arbitrary design variables and use its fundamental structure as



SW_CP_analysis.png

Fig. 2. Simplified representation of modeling a coupled slow-wave coplanar waveguide.

shown in Fig. 1 and simulated in a 2.5D EM simulator. Apart from the fundamental structure, we had also analyzed another structure where two metal layers were electrically connected with vias for the signal lines as shown in Fig. 3. The modified structure gave lower inductances and capacitances per unit length. The changes in L_{odd} , L_{even} , C_{odd} , C_{even} , Z_{0o} , and Z_{0e} for different geometric parameters of the CS-CPW are shown in Fig. 4. These variations are tabulated in Table I with the indicators showing increasing (\uparrow), decreasing (\downarrow), and no changing (∇) states over the changes in geometric parameters.

This behavior analysis gives a reasonable first approxima-

tion of selecting the design variables for the EM simulation. For an example, consider a case where we want to obtain a ratio of 1:6 for the odd- and even-mode impedances. It is evident from Fig. 4 and Table I that all the geometric parameters except the SG and GW have the influence on both the odd- and even-mode impedances. Therefore, for an initial guess to obtain such a large ratio, we must choose a minimum possible gap S between the signal lines. Moderate values can be chosen for the W and D and since the even-mode return current paths are defined to the side-ground lines, the even-mode impedances can be controlled by varying the SG and GW

TABLE I
MAPPING TABLE TO OBSERVE THE VARIATION OF L_{even} , L_{odd} , C_{even} , C_{odd} , Z_{0e} , AND Z_{0o} VS. GEOMETRICAL PARAMETER CHANGES

Geometrical parameter	Output					
	L_{even}	L_{odd}	C_{even}	C_{odd}	Z_{0e}	Z_{0o}
$W \uparrow$	\downarrow	\downarrow	\uparrow	\uparrow	\downarrow	\downarrow
$S \uparrow$	\downarrow	\uparrow	\uparrow	\downarrow	\downarrow	\uparrow
$D \uparrow$	\uparrow	\uparrow	\downarrow	\downarrow	\uparrow	\uparrow
$SG \uparrow$	\uparrow	\downarrow	\downarrow	\downarrow	\uparrow	\downarrow
$GW \uparrow$	\downarrow	\downarrow	\uparrow	\downarrow	\downarrow	\downarrow

without affecting the odd-mode impedances. This property of CS-CPW gives a great design flexibility.

Alternatively, instead of speculating the initial design variables from the behavior of the structure, one can obtain a mathematical model of the behavior of the structure using the simulation data. Then optimize the mathematical model to find the initial design variables. In the following section, we do linear regression to find a linear model and linear programming to optimize the linear model. We take the output of the linear program as the values of the initial design variables.

IV. MATHEMATICAL MODEL FOR ESTIMATING THE DESIGN PARAMETERS

For the sake of simplicity, let us change the variable notations from W , S , D , GW , and SG to x_1, x_2, x_3, x_4 , and x_5 respectively. The two critical positive outputs Z_{0e} and Z_{0o} to $y_1, y_2 \in \mathbb{R}$. We have learnt that y_1 is a function on 5 positive variables $x_1, x_2, x_3, x_4, x_5 \in \mathbb{R}$ and we name this function F . We also have learnt that y_2 is a function on 3 variables x_1, x_2, x_3 and we name this function G . Apart from being positive and real, the input variables have some other constraints depending on the used technology. We are interested to optimize the functions F and G while satisfying all the technology dependant constraints. We have been interested to optimize these functions in few alternative ways. The candidates are as follows:

- 1) Maximize $F - G$: Finding values $x_1 = a_1, x_2 = a_2, x_3 = a_3, x_4 = a_4, x_5 = a_5$ so that $F(a_1, a_2, a_3, a_4, a_5) - G(a_1, a_2, a_3)$ becomes as small as possible.
- 2) Minimize $|\frac{F}{G} - b|$: Finding values $x_1 = a_1, x_2 = a_2, x_3 = a_3, x_4 = a_4, x_5 = a_5$ so that $\frac{F(a_1, a_2, a_3, a_4, a_5)}{G(a_1, a_2, a_3)}$ becomes as close as possible to a certain constant b (ratio of)
- 3) Minimize $|F - b_1| + |G - b_2|$: Finding values $x_1 = a_1, x_2 = a_2, x_3 = a_3, x_4 = a_4, x_5 = a_5$ so that $F(a_1, a_2, a_3, a_4, a_5)$ and $G(a_1, a_2, a_3)$ goes as close as possible to constant values b_1 and b_2 respectively.

We need a mathematical model of the functions F and G to do such optimizations. Let $f_i : \mathbb{R} \rightarrow \mathbb{R}$ be a function that takes the variable x as input while the other input variables x_j for $j \in \{1, \dots, 5\} \setminus i$ of F are kept at constant values i.e.,

$$f_i(x|a_1, \dots, a_{i-1}, x, a_{i+1}, \dots, a_5) = F(a_1, \dots, a_{i-1}, x, a_{i+1}, \dots, a_5) \quad (1)$$

TABLE II
ERRORS OF LINEAR MODELS

Model	Error percentage			
	Mean	Standard Deviation	Min	Max
f	2.209766	2.480924	0.5398369	9.525519
g	1.002286	1.329765	0.008706377	5.115356

We define the function $g_i : \mathbb{R} \rightarrow \mathbb{R}$ in the same way so that

$$g_i(x|a_1, \dots, a_{i-1}, x, a_{i+1}, \dots, a_5) = G(a_1, \dots, a_{i-1}, x, a_{i+1}, \dots, a_5) \quad (2)$$

From the result of the experiments, presented in Figure 4, it is evident that f_i and g_i are almost, if not exactly, linear functions. Motivated by this observation, we make an educated guess that both of the functions F and G are approximately linear. We do not provide an analytical argument to justify the linearity of Z_{0o} and Z_{0e} . Instead, we use linear regression on the 18 experimental results to find models $f : \mathbb{R}^5 \rightarrow \mathbb{R}$, $g : \mathbb{R}^3 \rightarrow \mathbb{R}$ where $f(x_1, x_2, x_3, x_4, x_5) \approx G(x_1, x_2, x_3, x_4, x_5)$ and $g(x_1, x_2, x_3) \approx G(x_1, x_2, x_3)$ and compute the training errors.

A. Linear Regression

We use linear regression on the 18 experimental results and find the linear models f and g . We have used the statistical programming tool R to do the linear regression. We obtain the following models f and g and their errors by running the source file `model.R`. The source file is added in the Appendix.

$$f(x_1, x_2, x_3, x_4, x_5) = -7.266 \cdot x_1 + 0.372 \cdot x_2 + 29.175 \cdot x_3 - 3.278 \cdot x_4 + 1.823 \cdot x_5 + 78.226 \quad (3)$$

$$g(x_1, x_2, x_3) = -5.477 \cdot x_1 + 4.640 \cdot x_2 + 4.290 \cdot x_3 + 24.343 \quad (4)$$

For an input $(x_1 = a_1, x_2 = a_2, x_3 = a_3, x_4 = a_4, x_5 = a_5)$, the error percentages of the models f and g are as follow

$$\frac{|f(a_1, a_2, a_3, a_4, a_5) - F(a_1, a_2, a_3, a_4, a_5)|}{F(a_1, a_2, a_3, a_4, a_5)} \times 100$$

$$\frac{|g(a_1, a_2, a_3) - G(a_1, a_2, a_3)|}{G(a_1, a_2, a_3)} \times 100$$

We compute the mean, standard deviation, minimum and maximum error percentages of the models f and g over all the 18 inputs and present in Table II. We reckon, these error percentages indicate that the underlying functions F and G are fairly linear and the obtained models f and g are fairly good linear approximations. We optimize F and G by optimizing f and g respectively. As F and G are not not exactly linear and our obtained models f and g are linear approximations, the optimal values obtained from the models f and g will have some errors comparing to the optimal values of F and G . We expect these errors to be similar to the errors of the models.

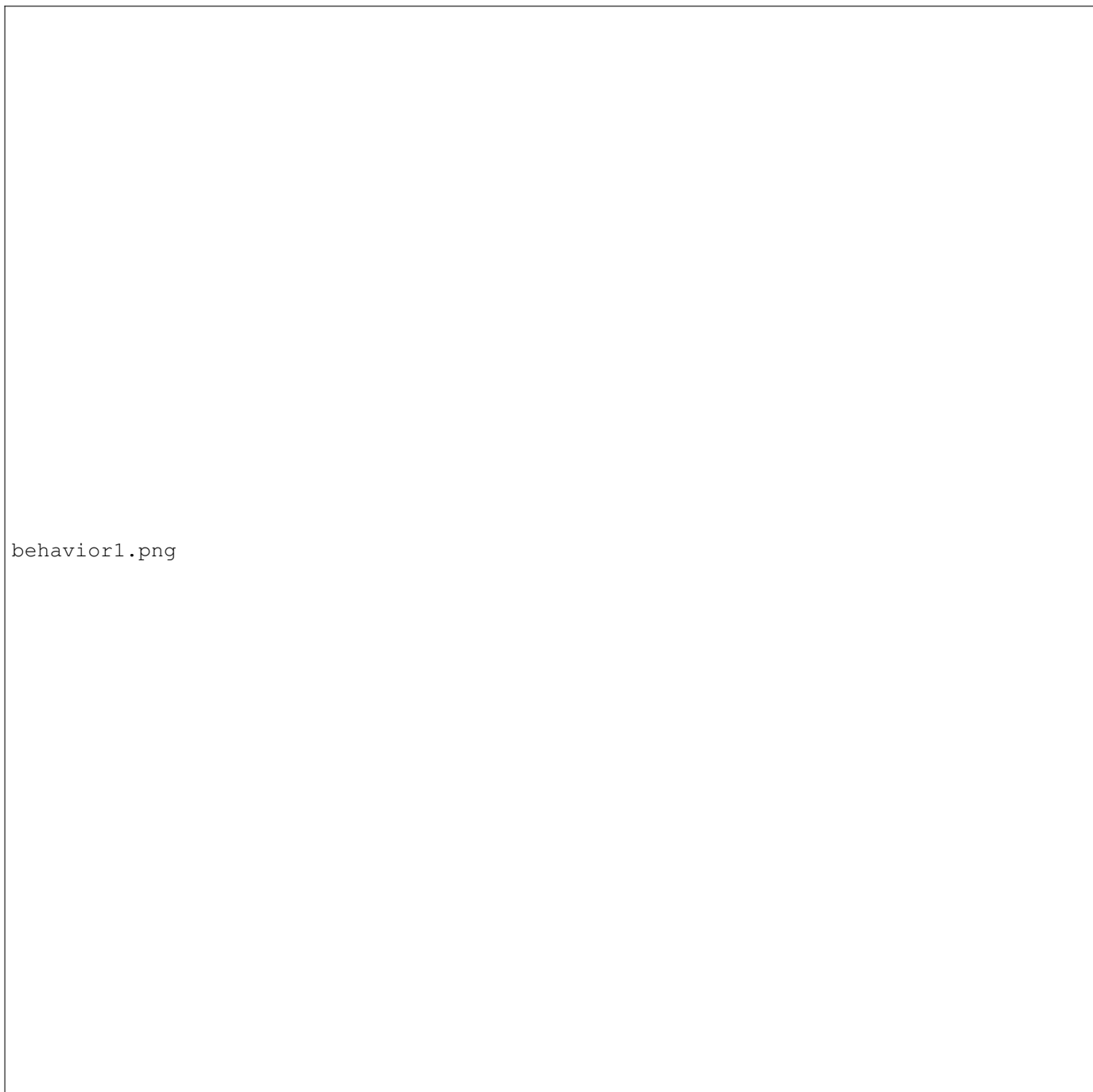


Fig. 4. Effect of the gap S , shielding distance D , signal width W , ground width GW , and signal to ground gap SG on the odd- and even-mode inductances (L_{odd} , L_{even}), capacitances (C_{odd} , C_{even}), and characteristic impedances (Z_{0o} , and Z_{0e}). Dotted lines represent the odd-mode and solid lines represent the even-mode line parameters.

B. Optimizing the Linear model Using Linear Programming:

As both f and g are linear and all the inputs of both of the functions are positive, the optimization problems are most likely to be representable as a linear programming problem. The linear programming problem would involve 5 variables. A linear programming problem with 5 variables is a small instance of a linear programming problem. There exist efficient algorithms, namely, simplex, ellipsoid, etc. for solving linear programming problems. In practice, a linear programming problem can easily be solved by any standard linear programming solver like `lp_solve`. Now we present the optimization problems discussed earlier as linear programming problems in the following subsections:

Maximize $f - g$: We need to find values $x_1 = a_1, x_2 = a_2, x_3 = a_3, x_4 = a_4, x_5 = a_5$ so that $f(a_1, a_2, a_3, a_4, a_5)$ becomes as large as possible while making $g(a_1, a_2, a_3)$ as small as possible, i.e., we need to maximize

$$\begin{aligned} f(x_1, x_2, x_3, x_4, x_5) - g(x_1, x_2, x_3) = & -1.7897 \cdot x_1 \\ & -3.9176 \cdot x_2 + 24.8859 \cdot x_3 - 3.2784 \cdot x_4 \\ & + 1.8231 \cdot x_5 + 53.8834 \end{aligned} \quad (5)$$

Consequently the linear programming problem looks as follows

$$\begin{aligned} \text{max:} \quad & -1.7897 \cdot x_1 - 3.9176 \cdot x_2 + 24.8859 \cdot x_3 \\ & -3.2784 \cdot x_4 + 1.8231 \cdot x_5 + 53.8834; \\ & x_1 \leq 11; x_2 \leq 6; x_3 \leq 2.04; \\ & x_4 \leq 11; x_5 \leq 20; x_1 \geq 2.5; \\ & x_2 \geq 1.5; x_3 \geq 1.25; x_4 \geq 4; \\ & x_5 \geq 10; \end{aligned}$$

The above linear programming problem can be solved by saving the above problem in a file named `model.lp` (the file is attached) and run the command `lp_solve model.lp` from the shell of an unix or unix like operating system. Here is the output:

- 1) We get the maximum value of the objective function to be: 117.648
- 2) The required values of the variables are $x_1 = 2.5, x_2 = 1.5, x_3 = 2.04, x_4 = 4, x_5 = 20$

Feeding this input to f and g we find

$$\begin{aligned} f(2.5, 1.5, 2.04, 4, 20) &= 143.4855 \\ g(2.5, 1.5, 2.04) &= 26.3621 \end{aligned}$$

We can find the value of $F(2.5, 1.5, 2.04, 4, 20)$ and $G(2.5, 1.5, 2.04)$ by running a simulation to see how good the optimization is.

Minimize $|\frac{f}{g} - b|$: We need to find the values $x_1 = a_1, x_2 = a_2, x_3 = a_3, x_4 = a_4, x_5 = a_5$ so that $\frac{f(a_1, a_2, a_3, a_4, a_5)}{g(a_1, a_2, a_3, a_4, a_5)}$ becomes as close as possible to a certain constant b . Let us set $b = 6$. Then we need to minimize $\frac{f(x_1, x_2, x_3, x_4, x_5)}{g(x_1, x_2, x_3)} - 6$. In

other words we need to minimize

$$\begin{aligned} & |f(x_1, x_2, x_3, x_4, x_5) - 6g(x_1, x_2, x_3)| \\ = & |25.5953 \cdot x_1 - 27.4675 \cdot x_2 + 3.4358 \cdot x_3 - \\ & 3.2784 \cdot x_4 + 1.8231 \cdot x_5 - 67.8316| \end{aligned}$$

The above simplification can be done easily for a different value of b than 6. However, for $b = 6$, the linear programming problem looks as follows. Note that a guest variable X has been imported in the linear program because the objective function involves an absolute value.

$$\begin{aligned} \text{min: } & X; \\ & x_1 \leq 11; x_2 \leq 6; x_3 \leq 2.04; \\ & x_4 \leq 11; x_5 \leq 20; x_1 \leq 2.5; \\ & x_2 \leq 1.5; x_3 \leq 1.25; x_4 \leq 4; \\ & x_5 \leq 10; \\ & 25.5953x_1 - 27.4675x_2 + 3.4358x_3 \\ & - 3.2784x_4 + 1.8231x_5 - 67.8316 \leq X; \\ & -25.5953x_1 + 27.4675x_2 - 3.4358x_3 + \\ & 3.2784x_4 - 1.8231x_5 + 67.8316 \leq X; \end{aligned}$$

Here is the output of the linear program:

- 1) We get the maximum value of the objective function to be: 0
- 2) The required values of the variables are $x_1 = 3.89215, x_2 = 1.5, x_3 = 1.25, x_4 = 4, x_5 = 10$

Feeding this input to f and g we find

$$\begin{aligned} f(3.89215, 1.5, 1.25, 4, 10) &= 92.08919 \\ g(3.89215, 1.5, 1.25) &= 15.34819 \end{aligned}$$

We can find the value of $F(3.89215, 1.5, 1.25, 4, 10)$ and $G(3.89215, 1.5, 1.25)$ by running a simulation to see how good the optimization is.

Minimize $|f - d_1| + |g - d_2|$: Finding the values $x_1 = a_1, x_2 = a_2, x_3 = a_3, x_4 = a_4, x_5 = a_5$ so that $f(a_1, a_2, a_3, a_4, a_5)$ and $g(a_1, a_2, a_3)$ goes as close as possible to constant values b_1 and b_2 respectively. Let us set $b_1 = 121$ and $b_2 = 20.7$. We need to minimize

$$\begin{aligned} & |f(x_1, x_2, x_3, x_4, x_5) - 121| + |g(x_1, x_2, x_3) - 20.7| \\ = & |-7.2667 \cdot x_1 + 0.3724 \cdot x_2 + 29.1759 \cdot x_3 \\ & - 3.2784 \cdot x_4 + 1.8231 \cdot x_5 - 42.7736| \\ & + |-5.477 \cdot x_1 + 4.640 \cdot x_2 + 4.290 \cdot x_3 + 3.643| \end{aligned}$$

The above simplification can be done easily for a different value of b_1 and b_2 . However, for $b_1 = 121$ and $b_2 = 20.7$, the linear programming problem looks as follows. Note that two guest variables X, Y has been imported in the linear program

because the objective function involves absolute value.

```

min: X + Y;
x1 <= 11; x2 <= 6; x3 <= 2.04; x4 <= 11; x5 <= 20;
x1 >= 2.5; x2 >= 1.5; x3 >= 1.25; x4 >= 4; x5 >= 10;
-7.2667x1 + 0.3724x2 + 29.1759x3
-3.2784x4 + 1.8231x5 - 42.7736 <= X;
7.2667x1 - 0.3724x2 - 29.1759x3
+3.2784x4 - 1.8231x5 + 42.7736 <= X;
-5.477x1 + 4.640x2 + 4.290x3 + 3.643 <= Y;
5.477x1 - 4.640x2 - 4.290x3 - 3.643 <= Y;

```

Here is the output of the linear program:

- 1) We get the maximum value of the objective function to be: 0
- 2) The required values of the variables are $x_1 = 3.5338, x_2 = 1.5, x_3 = 2.04, x_4 = 4, x_5 = 11.787$

Feeding this input to f and g we find

$$\begin{aligned}
 f(3.2077, 1, 1.25, 2.16454, 5) &= 121.0001 \\
 g(3.2077, 1, 1.25) &= 20.69998
 \end{aligned}$$

We can find the value of $F(3.2077, 1, 1.25, 2.16454, 5)$ and $G(3.2077, 1, 1.25)$ by running an simulation to see how good the optimization is.

C. Evaluation:

The underlying functions F and G of the experiments are found to be fairly linear. Keeping this observation in mind, linear approximation f and g can be obtained by linear regression by using only 5 experimental values. Because 5 points in a 5 dimensional space completely defines a 4 dimensional hyperplane. So, the linear approximations f and g can be easily obtained. Using the linear approximations, the above method can be used to find the values of the variables x_1, x_2, x_3, x_4, x_5 i.e., W, S, D, GW, SG to obtain the desired values of y_1 and y_2 i.e., Z_{0o} and Z_{0e} .

V. ALGORITHMIC DESIGN OF THE COUPLERS USING CS-CPW

In this section, we have described a step-by-step procedure to design a coupler using CS-CPW structure.

Step 1): At first, it is important to set the design goal. Depending on the coupler types, i.e. directional coupler with a certain coupling factor or 3-dB quadrature coupler the odd- and even-mode characteristic impedances are the key design parameters to be obtained. Fig. 5 shows a typical coupled-line coupler with its ports definition. It has been shown in the literature that the maximum coupling between the input port and the coupled port occurs at a frequency, when the lengths of the two identical parallel lines are quarter wavelengths at that frequency [R.Mongia]. Standard mathematical equations to calculate the required odd- and even-mode characteristic impedances for the coupled-line coupler are derived in [R. Mongia] shown in Eq. 1 and 2. Alternatively, an ideal coupled

general_coupler.png

Fig. 5. Typical coupled-line coupler with its ports definition.

line model from the microwave circuit simulator Keysight's ADS [ADS] or AWR Microwave Office [MWO] can be used to simulate the required odd- and even-mode impedances.

$$Z_{0e} = Z_0 \sqrt{\frac{1+k}{1-k}} \quad (6)$$

$$Z_{0o} = Z_0 \sqrt{\frac{1-k}{1+k}} \quad (7)$$

Step 2): Once the design goal is determined, we have to make an initial guess of the geometric parameters for the EM simulation. A suitable initial guess of these parameters is critical since it will directly affect the total time required for the design task. As stated in the previous section that the behavior of the CS-CPW shown in Table I or the mathematical modeling approach described in the previous section can be used to predict the initial values of the geometric parameters.

Step 3): An efficient EM simulation methodology is important to simulate the CS-CPW structure as the structure has five design variables. As a result, a high number of iterations may require to achieve the given design goal. Therefore, the modeling methodology of CS-CPW structure explained in the section II is proposed for designing the couplers. Since the structure has been modeled using the transmission line parameters [Pozar], the proposed CS-CPW model is scalable in terms of the length. Hence for designing a quadrature coupler, we do not need to simulate at the quarter wavelength of the line but a fractional length of the line. This will further reduce the simulation time. On the other hand, it is also important to check the complete coupler performances, i.e. through, coupling, isolation, and directivity at the quarter wavelength of the line. However, if we simulate the quarter wavelength of the line, we will not be able to extract the reliable line

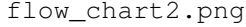


Fig. 6. Design flow of the couplers using CS-CPW.

parameters due to the resonance effect. Therefore, the scalable line parameters obtained from the EM simulations are inserted to a built-in physical coupled line model (CLINP) from the microwave circuit simulator ADS [ADS] for the complete coupler simulations.

Step 4): For this CS-CPW based coupler design approach, few iterations may require to obtain the given design goal although the behavior table will help significantly to reduce the number of iterations. If the design goal is not achievable with the fundamental structure of the CS-CPW even after few iterations then the structure can be modified based on the requirement. For an instance, in our design example (described in the next section) we have increased the coupling by modifying the signal lines of the CS-CPW for obtaining an aggressive odd-mode slow-wave effect.

Step 5): Finally, depending on the coupler applications, the signal lines can be folded in a similar fashion as in the Lange coupler to place the outputs or inputs on the same side. To finish the design, a complete coupler needs to be drawn in agreement with the design rules for the selected silicon technology. A flow-chart is shown in Fig. 6 to depict the design flow.

VI. E- TO W-BAND COUPLER DESIGN EXAMPLE

The proposed algorithm for designing CS-CPW based coupler was the basis of this design example. The design example had considered a 3-dB quadrature coupler which covers the entire E- and W-band. For a 3-dB quadrature coupler, the voltage coupling coefficient, k is calculated to be 0.708. Hence, by using the Eq. 1 and 2, the odd- and even-mode impedances become $Z_{0o} = 20.67 \Omega$, and $Z_{0e} = 120.9 \Omega$ for a 50Ω system. As mentioned in the design algorithm, the initial design parameters for the EM simulations can be

estimated from the Table I or the mathematical model. In this work, we had experimented both types of approaches. The experimental data obtained during the behavior analysis of the CS-CPW were used for the mathematical modeling and the design rules from the technology were applied for the boundary conditions. The design parameters estimated from the both approaches and their possible outcomes are tabulated in Table III. Implementable physical dimensions from the estimated values were used for the corresponding EM simulations. Because of the required values of Z_{0o} and Z_{0e} , the CS-CPW structure shown in Fig. 3 was preferred in the initial design phase. A fractional line length of $110 \mu\text{m}$ was considered for the EM simulations.

It can be seen from the Table III that the EM simulations using the design parameters obtained from the mathematical model had given better coupling coefficient. Therefore, these design parameters were used as initial values for the optimization iterations. However, EM simulations results using the values speculated from the behavioral table were also close to the design goal. The required coupling coefficient was achieved with single iteration; but the exact value of Z_{0o} and Z_{0e} could not be obtained. Note that this solution will sacrifice input match for coupling, as the port impedance is defined by, $Z_0 = \sqrt{Z_{0o}Z_{0e}}$ and that is $\sim 55 \Omega$. Nevertheless, we had drawn the layout of the coupler structure with these geometric parameters in the CMOS technology. However, the layout experienced metal density errors. In order to fulfill the metal density requirement, we had placed all the metal layers down to the shielding metal plane under the even-mode ground paths as shown in Fig. 7. However, this modification had large impact on even-mode line parameters, as was expected (even-mode return current paths are defined to the side-ground lines). In contrast, the even-mode slow-wave effect was increased significantly which had reduced the required coupler length. Simulation data showing these effects are also included in the Table III.

Due to the technology specific design rules constrain, the required coupling coefficient cannot be achieved with the straight forward CS-CPW structure shown in Fig. 7. Therefore, we had applied an engineering approach to obtain the design goal by introducing a special structure. While approaching to this particular structure, two things were considered. First, it was obvious that there were little room left to tune the even-mode line parameters, and second, the odd-mode slow-wave effect was less. Hence, we had modified the top most metal layer of the signal lines and created slabs for gaining strong capacitive coupling in odd-mode propagation as shown in Fig. 8. The new CS-CPW structure had provided high odd-mode effective dielectric constant and significantly lowered the odd-mode impedance while the changes in even-mode parameters were less prominent. The odd- and even-mode line parameters for this modified structure are also included in the Table II. The structure was built such a way that the CS-CPW remains scalable. We had considered the structure block as a unit cell so that the complete coupler structure can be made by repeating the number of required unit cells. In order to validate the scalability of the modified structure, we have simulated the structure with different number of unit cells and observe the

TABLE III
EM SIMULATED ODD- AND EVEN-MODE LINE PARAMETERS @90 GHZ FOR DIFFERENT GEOMETRIC PARAMETERS

Simulation scenario	Design parameter (μm)					Z_{0o} (Ω)	Z_{0e} (Ω)	k	ε_{ro}	ε_{re}	α_o (dB/m)	α_e (dB/m)	Complete coupler length (μm)
	W	S	D	GW	SG								
Estimated model from Table I	6	1.5	1.6	10	15	—	—	—	—	—	—	—	—
EM Simulated model	6	1.5	1.66	10	15	20.38	97	0.65	6	9.52	—	—	—
Mathematical model	3.53	1.5	2.04	4	11.8	20.7	121	0.71	—	—	—	—	—
EM Simulated model	3.5	1.5	2.04	4	12	23.4	130.5	0.69	5.1	6.3	1600	615	333
EM simulation iteration: 1	4	1.5	2.04	4	15	22.9	133	0.7	5.5	5.56	1860	600	340
EM simulation iteration: 2*	4	1.5	2.04	4	15	22.9	86.25	0.58	5.5	13.25	1860	670	275
EM simulation iteration: 3*	4	1.5	2.04	4	20	22.9	91.68	0.6	5.5	14.8	1860	700	260
EM simulation iteration: 4 [†]	4	1.5	2.04	4	20	12.7	93.45	0.76	23.8	15.35	4760	800	180
EM simulation iteration: 5 [†]	2.5	1.5	2.04	4	20	15.76	109	0.75	18.6	13.1	4760	865	200
EM simulation iteration: 6 [†]	2.5	1.5	1.57	4	20	16.73	105.7	0.73	17.5	13.6	4600	1240	205

*presence of all the metal layers under the even-mode ground paths

[†]with special structure



Fig. 7. Modified CS-CPW structure introduced for fulfilling the metal density requirements.



Fig. 8. Top view of CS-CPW structure when the signal lines are modified in odd-mode signal propagation. The unit cell is repeated N times to cover the complete coupler length. The slow-wave grids are not shown here to avoid any ambiguity in the figure.

effects on line parameters. It is understandable from Table III that the effect of repeating the unit cells on the line parameters are negligible hence the proposed structure is scalable.

Finally, the through port of the coupler was folded to its coupled port side for obtaining the in-phase and quadrature ports to the same side. The final geometric dimensions of the CS-CPW became $W = 2.5 \mu\text{m}$, $S = 1.5 \mu\text{m}$, $D = 1.54 \mu\text{m}$ (Metal 3), $SG = 19.75 \mu\text{m}$, $GW = 5 \mu\text{m}$. With these geometric dimensions the required metal density requirements needed for the circuit fabrication were fulfilled except for the metal 5 and 4. Therefore, extra metal plates on these two layers were placed and they had negligible effects on the line parameters. The final simulation structure in 3D view is shown in Fig. 9. The scalable line parameters obtained from the EM simulations are then used to predict the complete coupler performances and are shown in Fig. 10. From Fig. 10, it can be seen that the coupler has an insertion loss of -3.5 dB at

the coupling and through ports at 90 GHz, 18 dB of isolation, a less than 4° phase variations and a good matching over a wide bandwidth from 55 GHz to 110 GHz. It is noteworthy to observe that the coupler is critically-coupled even though the obtained coupling coefficient ($k = 0.73$) should give over-coupled performance. However, the simulation results were expected as the line loss was compensated by this extra coupling.

VII. MEASUREMENT RESULTS

The 3-dB quadrature coupler was fabricated in a 65-nm CMOS technology and the dimension is $56 \text{ mm} \times 205 \text{ mm}$. On-wafer S -parameter measurements were carried out for the coupler characterization. However, the coupled line coupler is a 4-port device and due the unavailability of the 4-port

TABLE IV
MY CAPTION

Odd-mode line parameters									
No. of unit cell	Corresponding R_{odd} Length (μm)	L_{odd} (Ω/mm)	C_{odd} (pH/mm)	G_{odd} (fF/mm)	Z_{0o} (S/mm)	ϵ_{ro} (Ω)	α_o (dB/mm)		
4	95.5	14	206.5	1283	0.002	12.7	23.8	4.76	
6	141.5	14.1	205.1	1305	0.004	12.6	24	4.86	
8	187.5	14.1	205	1320	0.006	12.6	24.3	4.88	
Even-mode line parameters									
No. of unit cell	Corresponding Length (μm)	R_{even} (Ω/mm)	L_{even} (pH/mm)	C_{even} (pH/mm)	G_{even} (S/mm)	Z_{0e} (Ω)	ϵ_{re}	α_e (dB/mm)	
4	95.5	18.1	1221	139	0.0001	93.45	15.35	0.795	
6	141.5	18	1220	139	0.0001	93.75	15.22	0.795	
8	187.5	18.03	1220	139	1.15E-04	93.7	15.24	0.883	

3D_figure_coupler_v1.png

coupler_simulation2.png

Fig. 9. 3D view of the final simulation structure for the coupler. The structure is $110 \mu\text{m}$ long and includes four unit cells and the through port is folded to the coupled port side.Fig. 10. Simulated S -parameters and phase difference between the through and coupled ports for the quadrature coupler.

VNA we had fabricated two exactly same coupler structures but with different port configurations for through and coupling measurement. For through measurement, the coupled and isolated ports were terminated to the on-chip 50Ω resistors and the input and through ports were connected to the probing pads. On the other hand, for coupling measurement the through and isolated port were terminated with 50Ω resistors and the input and coupled were connected to the probing pads. In order to facilitate the connection between a coupler port

and a probing pad an extra piece of SW-CPW of length $70 \mu\text{m}$ was added. The effects of the pads and the lines were de-embedded from the measurements by pad-short-open [DEumic11] and L-2L [L.2L] procedure, respectively. The micrograph of the coupler test structures are shown in Fig. 11. Measured and simulated results for the coupler are shown in Fig. 12. Good correlation is observed between simulations and measurements. However, slight over-coupling is observed in the measurements and that is because of the realized odd- and even-mode impedances were different than the targeted.

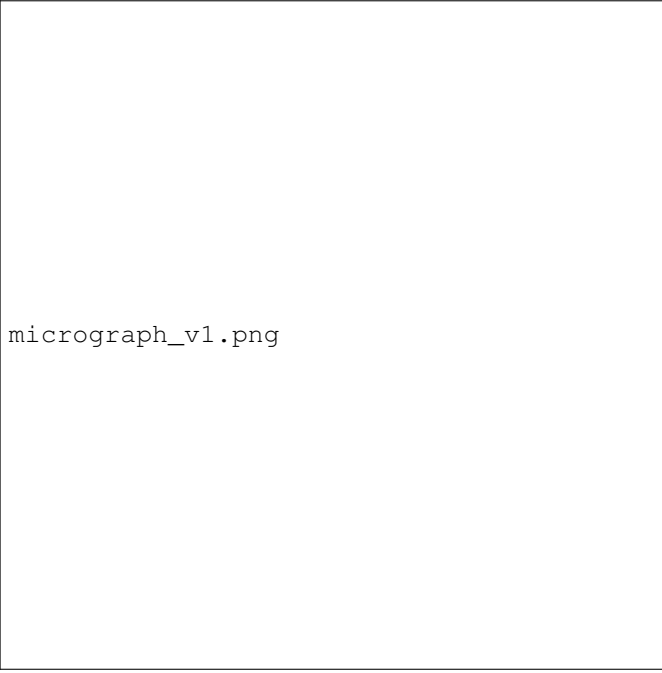


Fig. 11. Micrograph of the CS-CPW based coupler test structures for (a) through and (b) coupling measurements.

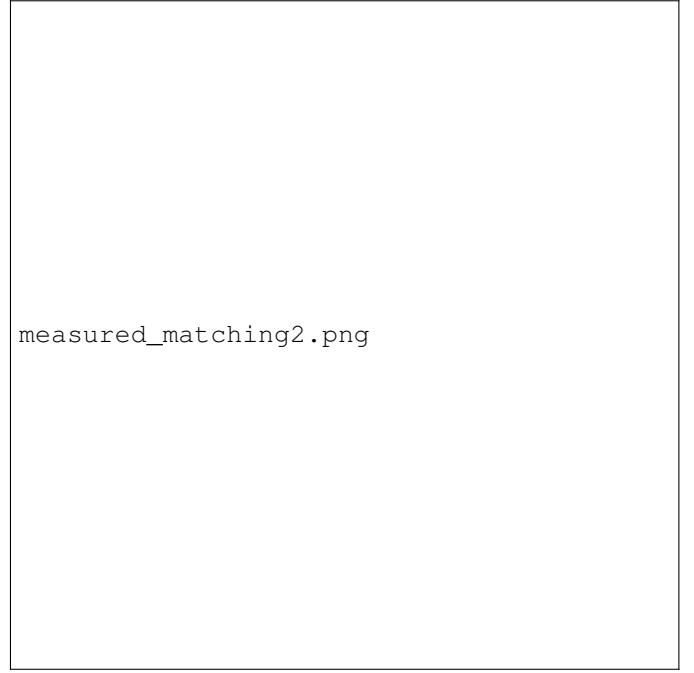


Fig. 13. Measured (dotted) and simulated (solid) performance of the matched coupler.



Fig. 12. Measured S -parameters and simulated and measured amplitude and phase errors for the E- to W- band coupler.

The measured coupler performance show an insertion loss of -3.5 dB at the through port and -4.4 dB at the coupled port at 90 GHz. A less than 2° phase variations, ± 1 -dB amplitude error, and better than 18 dB return loss is measured over a wide bandwidth from 55 GHz to 110 GHz.

Furthermore, too see the coupler performance without the de-embedding we had matched the coupler and fabricated two more structures as for the other case. For the matching, we had

modeled the pad and the SW-CPW through EM simulations, and terminated the isolated port with 38Ω . In this case, the length of the SW-CPW was $100 \mu\text{m}$. The measured and simulated matched coupler performances which include the pads and connecting transmission lines are shown in Fig. 13. Good agreement is again observed between measurements and simulations, especially the matching. However, the loss is bit higher than the simulation and this discrepancy may arise from the inaccurate pad modeling which is always difficult in mm-wave frequencies.

VIII. CONCLUSION

An algorithmic design methodology was developed for mm-wave CS-CPW based silicon couplers. Besides, an experiment on the behavior of the CS-CPW structure had performed and a design map has been created for improving the design efficiency. Based on the proposed design algorithm and the design map, a 3-dB quadrature coupler covering the whole E- to W-band has been successfully demonstrated in a 65-nm CMOS technology. The state-of-the-art results published for the 3-dB quadrature couplers realized on monolithic silicon technologies are shown in Table III. The presented results show excellent wideband coupler performances. A size reduction of about 50% compared to the conventional microstrip based quadrature couplers is achieved. Moreover, the good agreement between the simulation and measurement results indicates the validity of the applied modeling technique. The proposed CS-CPW based coupler is well suited for the design of compact mm-wave silicon radio front-ends.

APPENDIX A

PROOF OF THE FIRST ZONKLAR EQUATION

Appendix one text goes here.

TABLE V
STATE-OF- THE-ART PERFORMANCE OF MM-WAVE 3-DB QUADRATURE COUPLERS ON SILICON TECHNOLOGY

Ref	Topology	Technology	Frequency (GHz)	Insertion loss (dB)	Coupling (dB)	Return loss (dB)	± 1 dB BW (GHz)	± 5 BW (GHz)	Size(mm ²)
This work	CP-SW	65-nm CMOS	90	3.5	4.4	> 18	55	> 60	0.0115
[Floyd.IMS]	Lange coupler	130-nm BiCMOS	60	4	5	20	—	21*	0.048
[Floyd.IMS]	Lange coupler/meandering	130-nm BiCMOS	60	4	5	15	—	19*	0.0192
[D.Titz]	MBLC	130-nm BiCMOS	70	—	5.4	8.5	5	9	0.239
[D.Titz]	QLQC	130-nm BiCMOS	62	—	4.1	12.7	4	10.5	0.029
[EC.CPW]	EC-CPW	90-nm CMOS	62	4.8	5.5	22	~ 6.5	~ 9	0.102
[Ferrari.Thesis]	CP-SW	55-nm BiCMOS	60	3.3 ⁺	3.5 ⁺	29 ⁺	—	—	.069

APPENDIX B

Appendix two text goes here.

ACKNOWLEDGMENT

The authors would like to thank...

REFERENCES

- [1] H. Kopka and P. W. Daly, *A Guide to L^AT_EX*, 3rd ed. Harlow, England: Addison-Wesley, 1999.

PLACE
PHOTO
HERE

Dristy Parveg (S'09) received the B.Sc. degree in electrical and electronic engineering from the Rajshahi University of Engineering and Technology, Rajshahi, Bangladesh, in 2004, and the M.Sc. degree in electronic/telecommunications engineering from the University of Gvle, Gvle, Sweden, in 2009. He is currently pursuing the Ph.D. degree in electrical engineering with the Department of Electronics and Nanoengineering, Aalto University, Espoo, Finland. He was with Infineon Technologies Austria AG, Villach, Austria, from 2008 to 2009. His current research interests include millimeter-wave CMOS radio front-ends circuits for earth remote sensing applications and 5G communication.

Mikko Varonen (S'09) received the M.Sc., Lic.Sc., and D.Sc. (with distinction) degrees in electrical engineering from the Aalto University (formerly Helsinki University of Technology), Espoo, Finland, in 2002, 2005 and 2010, respectively. He is currently a Senior Scientist with the VTT Technical Research Centre of Finland, Espoo, Finland. During 2013 to 2016 he was an Academy of Finland Postdoctoral researcher with the Aalto University, Department of Electronics and Nanoengineering. During his postdoctoral fellowship, he was a Visiting scientist both at the Jet Propulsion Laboratory (JPL) and California Institute of Technology (EE), and Fraunhofer Institute of Applied Solid-State Physics. During 2013 to 2016 he was also with LNAFIN Inc., Helsinki, Finland. During 2011 he was a NASA Postdoctoral Program Fellow at the JPL. His research interests involve the development of millimeter-wave integrated circuits using both silicon and compound semiconductor technologies for applications ranging from astrophysics and Earth remote sensing to millimeter-wave communications.

Jane Doe Biography text here.